Source-receiver wave field interferometry

PHYSICAL REVIEW E **81**, 046601 (2010)

Source-receiver wave field interferometry

Andrew Curtis and David Halliday*
School of GeoSciences, The University of Edinburgh, Grant Institute, Kings Buildings, Edinburgh EH9 3JW, United Kingdom
(Received 30 June 2009; published 13 April 2010)

Correlation or convolution of recordings of diffuse fields at a pair of locations have been shown to result in estimates of the Green's function between the two locations. Variously referred to as wave field or seismic interferometry in different fields of research, Green's functions can thus be constructed between either pairs of receivers or pairs of energy sources. Proofs of these results rely on representation theorems. We show how to derive three acoustic and elastic representation theorems that unify existing correlational and convolutional approaches. We thus derive three forms of interferometry that provide Green's functions on source-to-receiver paths, using only energy that has propagated from surrounding sources or to surrounding receivers. The three forms correspond to three possible canonical geometries. We thus allow interferometric theory and methods to be applied to commonly used source-receiver configurations.

DOI: 10.1103/PhysRevE.81.046601 PACS number(s): 43.20.+g

I. INTRODUCTION

The field of wave field interferometry has grown dramatically in recent years. Developed most recently within the physics, acoustics, and geophysics communities (in the latter it is usually referred to as seismic interferometry), it has lead to schemas for Green's-function retrieval using background noise sources [1–5] and active or impulsive sources [6–8], for computational modeling of synthetic waveforms [9–11], and for noise removal [12–17].

The above interferometric advances were all made using a form of interferometry that uses cross-correlation, convolution, or deconvolution to convert recordings at a pair of receivers into derived data that would have been recorded had one of the two receivers been a source. We refer to this method as *inter-receiver* interferometry and think of the derived data as a wave field from a "virtual" (imagined) source at the location of one of the receivers and recorded by the other. By applying reciprocity to the results of van Manen *et al.* [9,10], Curtis *et al.* [12] also showed that Green's functions between pairs of source locations can be obtained by *inter-source* interferometry. Thus one constructs data as though one of a pair of sources had in fact been a receiver that recorded the signal from the other source. That study obtained seismograms (recordings of wave energy) from one earthquake energy source recorded on a virtual receiver (seismometer) constructed from, and at the location of, another earthquake source deep in the earth's subsurface.

Lobkis and Weaver [2] used modal theory to explain how Green's function are retrieved for diffuse noise fields. Wapenaar [18], van Manen *et al.* [9,10], and Wapenaar and Fokemma [19] used correlational forms of reciprocity theorems to show how inter-receiver Green's functions could be constructed by cross-correlating recorded fields. Slob *et al.* [7] and Wapenaar [20] showed that convolution could be applied to similar effect.

This paper presents a method to construct unified representation theorems that combine the correlational and convolutional forms used previously. The theorems are more general than their predecessors, allowing us to derive a third form of interferometry: source-receiver interferometry. Whereas the above studies convert receivers to virtual sources or sources to virtual receivers, the method converts real sources to virtual sources or real receivers to virtual receivers. Equivalently, it can be thought of as converting a real-source real-receiver pair to a virtual-receiver virtual-source pair, respectively. This is important as it allows various interferometric theories and methods to be applied to (more conventional) source-receiver configurations, which has not previously been possible. Applications include synthesizing data from new source-receiver paths in an existing experiment or survey, assessing the character of passive background noise fields, constructing an interferometric theory of source-receiver scattering, or facilitating data processing algorithms.

In this paper we derive both acoustic and elastic theory. Extension to a variety of other energy-propagation regimes including electromagnetic, electrokinetic, and diffusive propagation in attenuative, poroelastic or piezoelastic media seems relatively straightforward using a unified approach similar to Wapenaar *et al.* [21] and Snieder *et al.* [22].

II. UNIFIED REPRESENTATION THEOREM

We derive acoustic theory in the main text. An elastic version of the derivation below is given in Appendix A. Our starting points are the acoustic reciprocity theorems of both the convolution and correlation types. Each of these relates wave fields in two different states (e.g., due to two different energy source locations) and are given by [9,18,19]

$$\int_V \{p_A q_B - q_A p_B\} dV = \int_S \{p_A v_{i,B} - v_{i,A} p_B\} n_i dS \qquad (1)$$

and

$$\int_{V'} \{p_A^* q_C + q_A^* p_C\} dV' = \int_{S'} \{p_A^* v_{i',C} + v_{i',A}^* p_C\} n_{i'} dS', \qquad (2)$$

*Present address: Schlumberger Cambridge Research, High Cross, Cambridge CB3 0EL, United Kingdom.

respectively, where p_A is the acoustic pressure in state A, q_A is a source distribution in state A in terms of volume injection-rate density, $v_{i,A}$ is the ith component of particle velocity in state A, and * denotes complex conjugation. We have assumed there are no sources of the unidirectional point-force type (which would require extra volume integral terms), and these (and all following) expressions are formulated in the frequency domain and frequency dependence is implicit throughout. Surface S bounding volume V need not be the same as surface S' bounding volume V'.

By replacing one of the states A, B, or C by a Green's state we can derive the respective convolution-type and correlation-type representation theorems. We are free to choose any Green's state for either reciprocity theorem, and since Eqs. (1) and (2) are independent the Green's states in each of these equations need not be the same. We have, however, chosen to use one common state (A) in both equations to simplify derivations below.

We choose the following for state B in the convolution-type reciprocity theorem:

$$q_B(\mathbf{x}) = \delta(\mathbf{x}-\mathbf{x}_2), \quad p_B(\mathbf{x}) = G(\mathbf{x},\mathbf{x}_2),$$

$$v_{i,B}(\mathbf{x}) = \frac{-1}{j\omega\rho}\partial_i G(\mathbf{x},\mathbf{x}_2), \tag{3}$$

and the following for state C in the correlation-type reciprocity theorem:

$$q_C(\mathbf{x}') = \delta(\mathbf{x}'-\mathbf{x}), \quad p_C(\mathbf{x}') = G(\mathbf{x}',\mathbf{x}),$$

$$v_{i',C}(\mathbf{x}') = \frac{-1}{j\omega\rho}\partial_{i'} G(\mathbf{x}',\mathbf{x}). \tag{4}$$

Here $G(\mathbf{x},\mathbf{y})$ is the Green's function representing the pressure at $\mathbf{x}$ due to a volume injection-rate density source at location $\mathbf{y}$, ω is the angular frequency, ρ is the density at the source location (density is assumed to be constant from here on), the partial derivative ∂_i is taken with respect to the ith coordinate at the source location, and $j=\sqrt{-1}$. Using $v_i(\mathbf{x}) = (-1/j\omega\rho)\partial_i p(\mathbf{x})$ and choosing the states in Eqs. (3) and (4) allows Eqs. (1) and (2) to be rewritten as representation theorems:

$$p(\mathbf{x}_2) = \int_V G(\mathbf{x},\mathbf{x}_2) q(\mathbf{x}) dV + \frac{-1}{j\omega\rho}\int_S \{p(\mathbf{x}) n_i \partial_i G(\mathbf{x},\mathbf{x}_2) - n_i \partial_i p(\mathbf{x}) G(\mathbf{x},\mathbf{x}_2)\} dS \tag{5}$$

and

$$p^*(\mathbf{x}) = -\int_{V'} G(\mathbf{x}',\mathbf{x}) q^*(\mathbf{x}') dV' + \frac{-1}{j\omega\rho}\int_{S'} \{p^*(\mathbf{x}') n_{i'} \partial_{i'} G(\mathbf{x}',\mathbf{x}) - n_{i'} \partial_{i'} p^*(\mathbf{x}') G(\mathbf{x}',\mathbf{x})\} dS', \tag{6}$$

where the prime denotes that the integrals in Eq. (6) are over different domains compared to those in Eq. (5), and subscript A has been dropped from p and q since states B and C are now fully defined.

To combine the two Equations we substitute Eq. (6) into Eq. (5) and use source-receiver reciprocity $[G(\mathbf{x},\mathbf{x}_2) = G(\mathbf{x}_2,\mathbf{x})]$ to obtain

$$p(\mathbf{x}_2) = \int_V G(\mathbf{x},\mathbf{x}_2) q(\mathbf{x}) dV - \frac{-1}{j\omega\rho}\int_S \left\{ \left[\int_{V'} G^*(\mathbf{x}',\mathbf{x}) q(\mathbf{x}') dV' \right] n_i \partial_i G(\mathbf{x}_2,\mathbf{x}) - n_i \partial_i \left[\int_{V'} G^*(\mathbf{x}',\mathbf{x}) q(\mathbf{x}') dV' \right] G(\mathbf{x}_2,\mathbf{x}) + \left[\frac{-1}{j\omega\rho}\int_{S'} \{p(\mathbf{x}') n_{i'} \partial_{i'} G^*(\mathbf{x}',\mathbf{x}) - n_{i'} \partial_{i'} p(\mathbf{x}') G^*(\mathbf{x}',\mathbf{x})\} dS' \right] n_i \partial_i G(\mathbf{x}_2,\mathbf{x}) - n_i \partial_i \left[\frac{-1}{j\omega\rho}\int_{S'} \{p(\mathbf{x}') n_{i'} \partial_{i'} G^*(\mathbf{x}',\mathbf{x}) - n_{i'} \partial_{i'} p(\mathbf{x}') G^*(\mathbf{x}',\mathbf{x})\} dS' \right] G(\mathbf{x}_2,\mathbf{x}) \right\} dS. \tag{7}$$

This is a representation theorem that relates the pressure at $\mathbf{x}_2$ due to a source distribution defined by $q(\mathbf{x})$ to the pressure on the boundary S using Green's functions between points $\mathbf{x}'$ on the boundary S', points $\mathbf{x}$ on the boundary S, and point $\mathbf{x}_2$.

III. SOURCE-RECEIVER INTERFEROMETRY

We can show that this representation theorem is more general than existing theorems by deriving a form of interferometric integral that describes for the first time the construction of a real-source to real-receiver wave field. We now define the remaining source term to be $q(\mathbf{x}) = \delta(\mathbf{x}-\mathbf{x}_1)$ and hence the pressure to be $p(\mathbf{x}) = G(\mathbf{x},\mathbf{x}_1)$, the location $\mathbf{x}_2$ to be inside both boundaries S and S', and the location $\mathbf{x}_1$ to be outside the boundary S and inside the boundary S' [Fig. 1(a)]. Since $\mathbf{x}_1$ is outside of S, the integral over volume V in Eq. (7) is exactly zero, and integrals over volume V' result in

Green's functions from source location $\mathbf{x}_1$. The equation then becomes

$$
\begin{aligned}
G(\mathbf{x}_2,\mathbf{x}_1) = &-\frac{-1}{j\omega\rho}\int_S \{G^*(\mathbf{x}_1,\mathbf{x})n_i\partial_i G(\mathbf{x}_2,\mathbf{x}) \\
&- n_i\partial_i G^*(\mathbf{x}_1,\mathbf{x})G(\mathbf{x}_2,\mathbf{x})\}dS \\
&-\frac{-1}{j\omega\rho}\int_S \left\{\left[\frac{-1}{j\omega\rho}\int_{S'}\{G(\mathbf{x}',\mathbf{x}_1)n_{i'}\partial_{i'}G^*(\mathbf{x}',\mathbf{x})\right.\right. \\
&\left.\left. - n_{i'}\partial_{i'}G(\mathbf{x}',\mathbf{x}_1)G^*(\mathbf{x}',\mathbf{x})\}dS'\right] n_i\partial_i G(\mathbf{x}_2,\mathbf{x}) \right. \\
&\left. - n_i\partial_i\left[\frac{-1}{j\omega\rho}\int_{S'}\{G(\mathbf{x}',\mathbf{x}_1)n_{i'}\partial_{i'}G^*(\mathbf{x}',\mathbf{x})\right.\right. \\
&\left.\left. - n_{i'}\partial_{i'}G(\mathbf{x}',\mathbf{x}_1)G^*(\mathbf{x}',\mathbf{x})\}dS'\right] G(\mathbf{x}_2,\mathbf{x})\right\} dS.
\end{aligned}
\tag{8}
$$

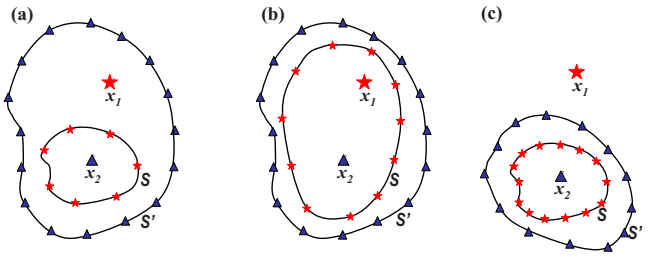

FIG. 1. (Color online) Canonical geometries. Triangles represent receivers, stars represent sources. S and S' are closed lines in two dimensions, surfaces in three dimensions.

The first integral on the right-hand side can be recognized as a cross-correlational form of seismic interferometry. Since $\mathbf{x}_1$ is outside and $\mathbf{x}_2$ is inside of boundary S, this integral gives the time reverse of the Green's function between $\mathbf{x}_1$ and $\mathbf{x}_2$ [compare Eqs. (19) and (20) in Slob *et al.* [7]]. Since time reversal is equivalent to complex conjugation in the frequency domain, we can therefore rewrite Eq. (8) as

$$
\begin{aligned}
G(\mathbf{x}_2,\mathbf{x}_1) + G^*(\mathbf{x}_2,\mathbf{x}_1) = &\frac{1}{j\omega\rho}\int_S \left\{\left[\frac{-1}{j\omega\rho}\int_{S'}\{G(\mathbf{x}',\mathbf{x}_1)n_{i'}\partial_{i'}G^*(\mathbf{x}',\mathbf{x}) - n_{i'}\partial_{i'}G(\mathbf{x}',\mathbf{x}_1)G^*(\mathbf{x}',\mathbf{x})\}dS'\right] n_i\partial_i G(\mathbf{x}_2,\mathbf{x})\right. \\
&\left. - n_i\partial_i\left[\frac{-1}{j\omega\rho}\int_{S'}\{G(\mathbf{x}',\mathbf{x}_1)n_{i'}\partial_{i'}G^*(\mathbf{x}',\mathbf{x}) - n_{i'}\partial_{i'}G(\mathbf{x}',\mathbf{x}_1)G^*(\mathbf{x}',\mathbf{x})\}dS'\right] G(\mathbf{x}_2,\mathbf{x})\right\} dS.
\end{aligned}
\tag{9}
$$

This is a formula that describes the recovery of a homogeneous Green's function (the Green's function plus or minus its time reverse) between a source at $\mathbf{x}_1$ and a receiver at $\mathbf{x}_2$ using only Green's functions from $\mathbf{x}_1$ to a surrounding boundary S' of receivers and Green's functions from a boundary S of sources that surrounds location $\mathbf{x}_2$. The integrals in square brackets describe a first step where the boundary S' is used to determine the Green's functions between the source at $\mathbf{x}_1$ and each source on the boundary S; hence this first step turns the source $\mathbf{x}_1$ into a virtual receiver. In a second step, the boundary S is used to determine the Green's function between the receiver at $\mathbf{x}_2$ and the newly generated virtual receiver $\mathbf{x}_1$. Thus this interferometric integral uses both surrounding sources and receivers to reconstruct source-receiver wave fields [Fig. 1(a)]. By applying energy sources at different locations [or simply by applying source-receiver reciprocity to Eq. (9)] it is possible to construct equivalent interferometric formulae with sources and receivers exchanged in a variety of configurations distributed between surfaces S' and S and locations $\mathbf{x}_1$ and $\mathbf{x}_2$ in Fig. 1(a).

It may seem contradictory that to obtain Eq. (7) we assume the medium to be source-free outside of S, then to obtain Eq. (8) we define the source field q to be nonzero at $\mathbf{x}_1$. However, in practice this can be resolved by ensuring that the emission of energy from the source at $\mathbf{x}_1$ is separated in time from emissions from sources on surface S.

To derive a more applicable form of the integral we might assume that the Sommerfield radiation conditions [23] hold on one or both bounding surfaces (these conditions are $\mp jkG = n_i\partial_i G$ with $-$ indicating outgoing waves and $+$ indicating incoming waves at the boundary; these conditions hold if waves travel perpendicularly to the boundaries). Assuming these conditions are approximately met on both boundaries reduces the integral to

$$
\begin{aligned}
&G(\mathbf{x}_2,\mathbf{x}_1) + G^*(\mathbf{x}_2,\mathbf{x}_1) \\
&\quad\approx \frac{4k^2}{(\omega\rho)^2}\int_S\int_{S'} G(\mathbf{x}',\mathbf{x}_1)G^*(\mathbf{x}',\mathbf{x})G(\mathbf{x}_2,\mathbf{x})dS'dS.
\end{aligned}
\tag{10}
$$

This result is the more precise equivalent of the particular case presented by Curtis [24] in which the Sommerfield conditions were assumed throughout the derivation. Hence, provided the Sommerfield radiation conditions are met, source-to-receiver interferometry can be applied as a double integral over the frequency domain product of three Green's functions.

The Sommerfield conditions require that the energy leaves the surfaces approximately perpendicularly, as would occur, for example, if each integration surface was a circle with large radius. This has previously been shown to provide rea-

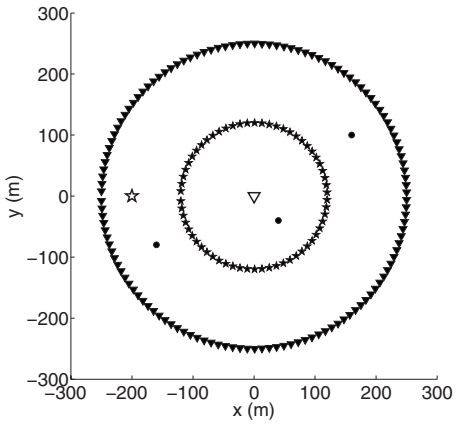

FIG. 2. Geometry used for the numerical example. Stars indicate sources, triangles indicate receivers, and dots indicate scatterers. Solid stars and triangles indicate boundary sources at locations $\mathbf{x}$, and boundary receivers at locations $\mathbf{x}'$, respectively, and the open star and triangle indicate the source at $\mathbf{x}_1$ and receiver at $\mathbf{x}_2$, respectively. Only every third boundary position is plotted for clarity.

sonable results in practical situations using both correlational and convolutional forms of interferometry. With two integration surfaces, one located inside the other, it may be more difficult for these conditions to be approximated in practice, and this should be considered whenever applying interferometry in the form presented by Eq. (10) rather than Eq. (9).

IV. NUMERICAL EXAMPLE

We now illustrate the source-receiver approach using a simple two-dimensional numerical example. We use a deterministic variation in Foldy's method [10,25] to compute synthetic acoustic wave fields in a multiply-scattering model. This method uses the optical theorem to correctly constrain the values of the scattering amplitudes such that energy is conserved. In this example we use a constant wave propagation velocity of 750 m/s, a unit density, and scatterers of equal strength. Computations are carried out in the frequency domain, but for visualization the results are plotted in the time domain. These time series are frequency-band limited from 0 to 60 Hz using a Ricker wavelet with a center frequency of 30 Hz. The geometry for the example is shown in Fig. 2. Stars indicate sources, triangles indicate receivers, and dots indicate scatterers. Note that the solid stars and triangles indicate boundary sources and receivers and the empty star and triangle indicate the source and receiver between which we wish to calculate the wave field. Only every third boundary position is plotted for clarity. Compare the source and receiver geometry in Fig. 2 with that in Fig. 1(a).

We now illustrate the application of Eq. (9) to calculate the source-receiver wave field, $G(\mathbf{x}_2,\mathbf{x}_1)+G^*(\mathbf{x}_2,\mathbf{x}_1)$. Rather than showing only the final result, we first show the intermediate step of solving the inner integral in square brackets in Eq. (9) for one boundary source (at $\mathbf{x}$) and the source at $\mathbf{x}_1$ [when we describe these as "inner" and "outer" integrals we are referring to their position in Eq. (9) rather than their physical position in Fig. 2]. In Fig. 3(a) we show the inner integrand for the boundary source at $[-120, 0]$ m. This integrand is summed over boundary receiver positions to give the solution of the inner integral for one source pair $(\mathbf{x},\mathbf{x}_1)$ [Fig. 3(b)]. This represents the result of the virtual-receiver method [12], where we effectively turn one of the sources at either $\mathbf{x}$ or $\mathbf{x}_1$ into a virtual receiver (recording both positive- and negative-time responses). This result is repeated for every source boundary position $\mathbf{x}$. Finally we use the results of the inner integral to solve Eq. (9) for the source-receiver wave field. In Fig. 4(a) we show the integrand of the outer integral (after evaluation of the inner integral) and in Fig. 4(b) we show the result of summing over all boundary sources; this is the source-receiver wave field $G(\mathbf{x}_2,\mathbf{x}_1)+G^*(\mathbf{x}_2,\mathbf{x}_1)$ in the time domain. Note that there is both a forward-time part and a reverse-time part (since the complex conjugation in the frequency domain corresponds to time reversal in the time domain). For reference the directly modeled (noninterferometric) result found using Foldy's method is shown by dots superimposed on Fig. 4(b). Apart from

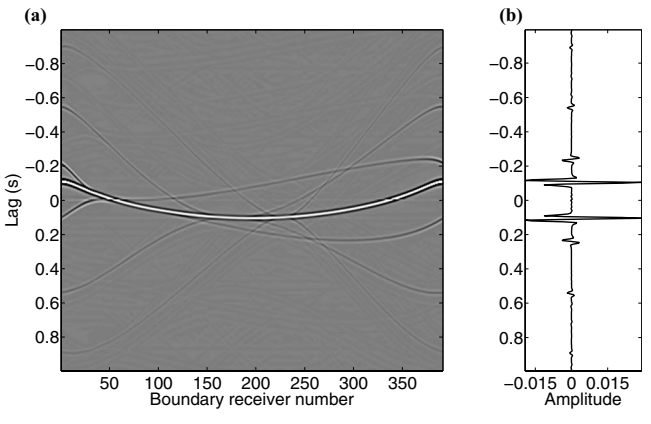

FIG. 3. (a) The inner integrand in Eq. (9) plotted for a single source pair $(\mathbf{x},\mathbf{x}_1)$. The boundary receiver number corresponds to the receivers at $\mathbf{x}'$, on the boundary S'. (b) Sum of (a) over boundary receiver number. This represents the solution of the inner integral for one source pair $\mathbf{x}$-$\mathbf{x}_1$.

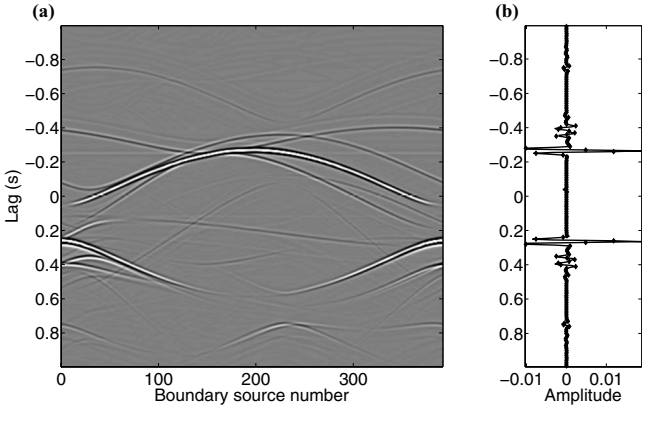

FIG. 4. (a) The outer integrand in Eq. (9) after the solution of the inner integral. The boundary source number corresponds to the sources, $\mathbf{x}$ on the boundary S. (b) Sum of (a) over boundary source number. This represents the solution of Eq. (9) for the source-receiver pair $(\mathbf{x}_1,\mathbf{x}_2)$. Dots overlying the signal represent the exactly-computed solution.

small numerical errors in the implementation these two results are identical.

V. DISCUSSION

Equation (9) is similar in form to the imaging condition presented by Oristaglio [26] who uses the Born approximation to derive a formula that relates direct and scattered waves to the scattering potential using a double integration like that in Eq. (9). He assumed that both surfaces of sources and receivers lay on a single boundary that surrounded both locations $\mathbf{x}_1$ and $\mathbf{x}_2$—requiring two correlational integrals in his derivation rather than one correlational and one convolutional as above. While his results differ, his approach suggests two further ways in which the representation theorems and corresponding interferometric integrals can be derived using a similar method to above.

A second representation theorem and interferometric formula can be obtained using the geometry shown in Fig. 1(b). In this case both source location $\mathbf{x}_1$ and receiver location $\mathbf{x}_2$ lie inside surface S of sources and surface S is itself surrounded by surface S' of receivers. Two correlational reciprocity theorems must therefore be used for states A, B, and C in Eqs. (1) and (2) [i.e., Eq. (1) is replaced by a correlational reciprocity relation]. Yet a third set of results can be derived for the geometry in Fig. 1(c) by starting with two convolutional reciprocity relations in place of Eqs. (3) and (4) and following similar steps in the derivation. The resulting representation theorems and interferometric relations for the two cases in Figs. 1(b) and 1(c) are given in Appendix B.

These are not the only geometrical variations that are possible. For example, S could surround only the receiver at $\mathbf{x}_2$ while S' surrounds only the source at $\mathbf{x}_1$, again resulting in a combination of two convolutional reciprocity relations. Nevertheless, the geometries shown in Fig. 1 are canonical in the sense that they span the three possible types of combinations: two correlational relations, two convolutional relations, and one of each.

The relation in Eq. (10) synthesizes the Green's function on the $\mathbf{x}_1$ to $\mathbf{x}_2$ source-receiver path using only Green's functions from and to surrounding sources and receivers, respectively. It is approximate because only monopolar (e.g., explosive) sources are included. The exact relationship in Eq. (9) also requires dipolar (strain rather than displacement) sources which are often not available in practical experiments. Also, the Green's-function estimates obtained are diffraction limited in the sense defined by de Rosny and Fink [27] ; this only affects the accuracy of results if locations $\mathbf{x}_1$ and $\mathbf{x}_2$ are less than a wavelength apart.

In practical experiments it is not often the case that one can acquire data using sources and receivers located in closed surfaces such as S and S' in Fig. 1(a). Snieder [28] showed that for approximately homogeneous background media, the integrand of correlational interferometric integrals such as the integral over receivers on S in Eqs. (9) and (10) only integrates constructively over parts of S spanned by open hyperbolic shapes such as those depicted in Fig. 5(a) (see also [17,29,30]). A similar analysis for convolutional interferometry shows that the integral over S' is only constructive over parts of S' spanned by the central elliptical region in Fig. 5(b). Hence, provided the medium is not too heterogeneous, in practice we can limit the source and receiver geometry to that shown in Fig. 5(c). For this geometry, Fig. 6 shows the various sets of Green's functions used in Eq. (10) to create an approximation to the Green's function between $\mathbf{x}_1$ and $\mathbf{x}_2$ [taking the mirror image of boundary S' and all ray paths in Fig. 6 about surface S accounts for the other section of S' shown in Fig. 5(c)]. It is of course also possible to use source-receiver reciprocity to reverse the role of sources and receivers in all of the above. In that case, all sources in Figs. 1, 5, and 6 should be swapped for receivers and vice versa.

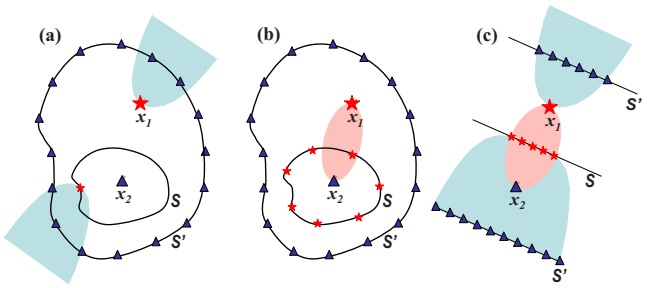

FIG. 5. (Color online) Regions of stationary phase within the interferometric integrals corresponding to the geometry shown in Fig. 1(a). Key as in Fig. 1. Shaded hyperbolae show stationary phase regions for correlational interferometry, while ellipses show the same for convolutional interferometry.

There are several applications for which it might be useful to turn a real source into a virtual source. First, notice that the source-receiver record between $\mathbf{x}_1$ and $\mathbf{x}_2$ is obtained using only the other source-receiver Green's functions illustrated in Fig. 6. This means that if the latter records are available, the source-receiver record between $\mathbf{x}_1$ and $\mathbf{x}_2$ can be synthesized without having to measure it directly. This might be useful, for example, if the receiver at $\mathbf{x}_2$ had not been activated when the source at $\mathbf{x}_1$ was fired but had been activated by the time shots on surface S were fired. Thus, new source-receiver paths can be synthesized and added to existing surveys or experiments without the need to acquire further data.

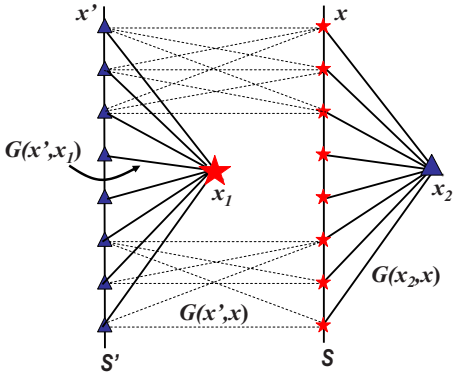

FIG. 6. (Color online) Graphical representation of the three measured sets of Green's functions used in Eq. (10). Symbol key as in Fig. 1.

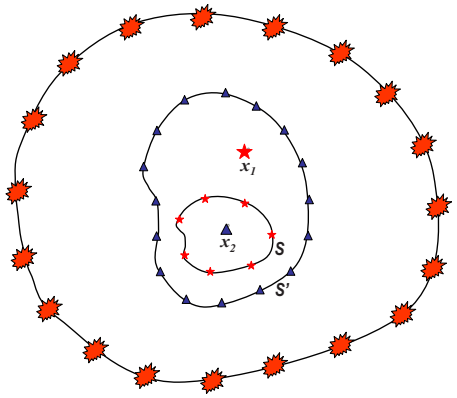

FIG. 7. (Color online) A geometry for which interferometry using both active (stars) and passive (flashes) sources is possible. Other symbols as in Fig. 1.

It is possible that all of the above theory could be used with only passive noise energy sources. Wapenaar and Fokkema [18,19] showed that Green's functions between any two receivers could be estimated using extended recordings of such (uncorrelated) noise by simply carrying out cross-correlations similar to the inner surface integral in Eq. (9). If, for example, we place sources on the outer boundary S' in Fig. 1(b) and put receivers at all of the other interior locations marked in that figure, all of the Green's functions used in Eq. (B2) in Appendix B [the equivalent form to Eq. (9), but for the geometry in Fig. 1(b)] can be estimated and hence so can the (inter-receiver) Green's functions between locations $\mathbf{x}_1$ and $\mathbf{x}_2$. However, in that case the inter-receiver Green's function between $\mathbf{x}_1$ and $\mathbf{x}_2$ can also be estimated directly by using inter-receiver interferometry. Hence, there are now two possible ways to estimate this latter Green's function interferometrically.

Notice that it is therefore similarly also possible that different sets of the various Green's functions involved in Eq. (9) can be obtained using different types of energy sources. For example, the Green's functions between the receiver at point $\mathbf{x}_2$ and receivers on boundary S' in Fig. 1(a) could be estimated using (active or) passive noise sources (spanning some third, external surface surrounding surface S' as in Fig. 7. Equation (9) or Eq. (10) could then be used to combine these with active source data that provided recordings of Green's functions between $\mathbf{x}_1$ and S' and between points on S and S' to obtain finally the Green's function between $\mathbf{x}_1$ and $\mathbf{x}_2$. Thus we show for the first time how passive and active wave field data can be combined effectively within a single interferometric application.

Similarly, note that if the Green's function between $\mathbf{x}_1$ and $\mathbf{x}_2$ had been recorded using an active source at $\mathbf{x}_1$, in addition to all other Green's functions shown in Fig. 6, then the new interferometric relations identify redundancy in the acquired data. Such redundancy is often useful, for example, to assess the accuracy of data recordings by comparing measured and synthesized wave fields between $\mathbf{x}_1$ and $\mathbf{x}_2$.

There are also situations in which recordings from both an active and a virtual source enable subsequent methods that are otherwise impossible. An example is the surface wave removal method of Curtis *et al.* [12], Dong *et al.* [13], and Halliday *et al.* [14]. These methods make use of the fact that interferometric estimates of Green's functions between two points, synthesized using energy from surrounding sources on a free surface, tend to be dominated by surface waves. If a real source-receiver record also exists between the same two points, the interferometric estimate can be adaptively subtracted from the real record to leave a data set with surface waves removed. This is desirable for example when using reflection seismology to image the earth's subsurface since surface waves recorded at typical industrial frequencies only contain information about the shallow subsurface, whereas targets of interest are often relatively deep. In such cases the surface wave energy usually masks target reflections, hence its removal is advantageous. This method clearly requires both virtual and real sources from the same point ($\mathbf{x}_1$) recorded at the same receiver (at $\mathbf{x}_2$). To obtain such records using either inter-source or inter-receiver interferometry would require the colocation of receivers at every source point, which is not economical in seismic surveys. Using source-receiver interferometry, however, the virtual-source record can be synthesized from the real source using records that might usefully be recorded in a land seismic survey anyway. The same may also apply in a marine setting where free-surface multiples are to be removed from active source data.

Another application is to create a method to characterize the effectiveness of seismic interferometry. For a particular source and receiver geometry on surfaces S and S' we might wish to assess the extent to which interferometry could be used to synthesize new records with some existing, theoretically imperfect geometry of surrounding energy sources. If a real source and receiver were placed at $\mathbf{x}_1$ and $\mathbf{x}_2$, respectively, the recorded trace from the real source could be compared to that constructed by interferometry using Eqs. (9) and (10). Similarly to above, the only previously existing way to make a direct comparison would be to colocate a receiver with the source and use inter-receiver interferometry to construct the comparison record; however, such comparisons would be affected by differences between the radiation pattern of the source and the spatiotemporal sensitivity of the receiver. Using the new method we remove any such effects since the same source is used for both compared records.

From a theoretical point of view, the theory presented here also provides a sound basis for schemes to correct biases in wave field interferometry such as those observed using the above method of comparison. For example, Curtis and Halliday [31] present a data driven method to correct such biases using a locally dense array of measurements around the location $\mathbf{x}_2$. The interferometrically constructed Green's functions between $\mathbf{x}_2$ and each point in the local array are compared to a desired (e.g., isotropic) source radiation pattern, and correction factors thus derived are used to correct the Green's-function estimate between $\mathbf{x}_2$ and $\mathbf{x}_1$. The geometries used in that paper are essentially similar to those in Fig. 1(a) although some of the sources and receivers are exchanged (surface S' is spanned by sources, and all locations interior to S' are spanned by receivers). Hence, initially Curtis and Halliday correct Green's functions between $\mathbf{x}_2$ and each point on a local surface S around $\mathbf{x}_2$ to some predefined, desired form. However, in that paper the algorithm

used to apply the resulting correction factors was established heuristically, whereas Eq. (10) herein provides an exact basis with which to obtain the Green's function between $\mathbf{x}_2$ and $\mathbf{x}_1$ given corrected Green's functions between $\mathbf{x}_2$ and each point on S.

Finally, the theoretical developments presented here have also been extended to derive an interferometric theory of scattering on source-receiver paths (Halliday and Curtis [32]) by using the scattering reciprocity theorems of Vasconcelos *et al.* [33]. This interferometric scattering theory is shown to be a generalization of the theory of Oristaglio [26] who derives an inverse Born-scattering formula based on the solution of two integrals similar to those in Eq. (9). Halliday and Curtis [32] showed that the perturbed form of source-receiver interferometry generalizes Oristaglio's theory to nonlinear, multiple-scattering regimes.

The above applications may be representative of current practice. However, wave field interferometry is a field that is developing rapidly. Hence, it is likely that the theorems and relations derived herein will find application in many areas currently unforeseen.

VI. CONCLUSIONS

We have derived three representation theorems, describing the wave field at one point due to sources and receivers on two surrounding boundary surfaces. We use these theorems to derive three interferometric relations that describe the construction of a wave field between a source and a receiver using only Green's functions from and to surrounding boundaries of sources and receivers. Finally, we have shown how the method could be applied in practice when either the geometry or types of sources and receivers may be more limited than is required by the exact theory.

APPENDIX A: AN EXAMPLE ELASTIC DERIVATION

We now derive the elastic equivalent of the theorem described in the main text. We begin with the representation theorems of both the convolution type and the correlation type [10,34]:

$$u_i(\mathbf{x}_2) = \int_V G_{in}(\mathbf{x}_2,\mathbf{x}) f_n(\mathbf{x}) dV + \int_S \{G_{in}(\mathbf{x}_2,\mathbf{x}) n_j c_{njkl} \partial_k u_l(\mathbf{x}) - n_j c_{njkl} \partial_k G_{il}(\mathbf{x}_2,\mathbf{x}) u_n(\mathbf{x})\} dS, \tag{A1}$$

$$u_i^*(\mathbf{x}) = \int_{V'} G_{in'}(\mathbf{x},\mathbf{x}') f_{n'}^*(\mathbf{x}') dV' + \int_{S'} \{G_{in'}(\mathbf{x},\mathbf{x}') n_{j'} c_{n'j'k'l'} \partial_{k'} u_{l'}^*(\mathbf{x}') - n_{j'} c_{n'j'k'l'} \partial_{k'} G_{il'}(\mathbf{x},\mathbf{x}') u_{n'}^*(\mathbf{x}')\} dS', \tag{A2}$$

where $u_i(\mathbf{x}_2)$ is the ith component of particle displacement at $\mathbf{x}_2$, $G_{in}(\mathbf{x}_2,\mathbf{x})$ is the Green's function representing the ith component of particle displacement at $\mathbf{x}_2$ due to a unidirectional point force in the n direction at $\mathbf{x}$, $f_n(\mathbf{x})$ is a force in the n direction at $\mathbf{x}$, n_j is the jth component of the normal vector on the boundary S, ∂_k denotes a spatial derivative in the k direction, and c_{njkl} is the stress tensor. Primed and unprimed quantities indicate that these relate to the primed and unprimed boundaries, respectively.

To combine the two equations we substitute Eq. (A2) into Eq. (A1):

$$u_i(\mathbf{x}_2) = \int_V G_{in}(\mathbf{x}_2,\mathbf{x}) f_n(\mathbf{x}) dV + \int_S \left\{ G_{in}(\mathbf{x}_2,\mathbf{x}) n_j c_{njkl} \partial_k \left[\int_{V'} G_{ln'}^*(\mathbf{x},\mathbf{x}') f_{n'}(\mathbf{x}') dV' \right] - n_j c_{njkl} \partial_k G_{il}(\mathbf{x}_2,\mathbf{x}) \times \left[\int_{V'} G_{nn'}^*(\mathbf{x},\mathbf{x}') f_{n'}(\mathbf{x}') dV' \right] \right\} dS + \int_S \left\{ G_{in}(\mathbf{x}_2,\mathbf{x}) n_j c_{njkl} \partial_k \left[\int_{S'} \{G_{ln'}^*(\mathbf{x},\mathbf{x}') n_{j'} c_{n'j'k'l'} \partial_{k'} u_{l'}(\mathbf{x}') - n_{j'} c_{n'j'k'l'} \partial_{k'} G_{ll'}^*(\mathbf{x},\mathbf{x}') u_{n'}(\mathbf{x}')\} dS' \right] - n_j c_{njkl} \partial_k G_{il}(\mathbf{x}_2,\mathbf{x}) \left[\int_{S'} \{G_{nn'}^*(\mathbf{x},\mathbf{x}') n_{j'} c_{n'j'k'l'} \partial_{k'} u_{l'}(\mathbf{x}') - n_{j'} c_{n'j'k'l'} \partial_{k'} G_{nl'}^*(\mathbf{x},\mathbf{x}') u_{n'}(\mathbf{x}')\} dS' \right] \right\} dS. \tag{A3}$$

This representation theorem relates the particle displacement at $\mathbf{x}_2$ to the particle displacement on the boundary S' using Green's functions between the boundary S', the boundary S, and $\mathbf{x}_B$.

We can show that this elastodynamic representation theorem is more general than existing theorems by deriving a form of interferometric integral that describes the construction of a real-source to real-receiver wave field in elastic media. We now define the remaining source term to be $f_i(\mathbf{x}) = \delta_{im}\delta(\mathbf{x}-\mathbf{x}_1)$ and hence the particle displacement to be $u_i(\mathbf{x}) = G_{im}(\mathbf{x},\mathbf{x}_1)$, the location $\mathbf{x}_2$ to be inside both boundaries S and S', and the location $\mathbf{x}_1$ to be outside the boundary S and inside the boundary S' [Fig. 1(a)]. Since $\mathbf{x}_1$ is outside of S, the integral over volume V in Eq. (A3) is exactly zero, and integrals over volume V' result in Green's functions from source location $\mathbf{x}_1$. The equation then becomes

$$G_{im}(\mathbf{x}_2,\mathbf{x}_1) = \int_S \{G_{in}(\mathbf{x}_2,\mathbf{x}) n_j c_{njkl} \partial_k G^*_{lm}(\mathbf{x},\mathbf{x}_1) - n_j c_{njkl} \partial_k G_{il}(\mathbf{x}_2,\mathbf{x}) G^*_{nm}(\mathbf{x},\mathbf{x}_1)\} dS$$
$$+ \int_S \left\{ G_{in}(\mathbf{x}_2,\mathbf{x}) n_j c_{njkl} \partial_k \left[\int_{S'} \{G^*_{ln'}(\mathbf{x},\mathbf{x}') n_{j'} c_{n'j'k'l'} \partial_{k'} G_{l'm}(\mathbf{x}',\mathbf{x}_1) - n_{j'} c_{n'j'k'l'} \partial_{k'} G^*_{ll'}(\mathbf{x},\mathbf{x}') G_{n'm}(\mathbf{x}',\mathbf{x}_1)\} dS' \right] \right.$$
$$\left. - n_j c_{njkl} \partial_k G_{il}(\mathbf{x}_2,\mathbf{x}) \left[\int_{S'} \{G^*_{nn'}(\mathbf{x},\mathbf{x}') n_{j'} c_{n'j'k'l'} \partial_{k'} G_{l'm}(\mathbf{x}',\mathbf{x}_1) - n_{j'} c_{n'j'k'l'} \partial_{k'} G^*_{nl'}(\mathbf{x},\mathbf{x}') G_{n'm}(\mathbf{x}',\mathbf{x}_1)\} dS' \right] \right\} dS. \tag{A4}$$

As in the main text, the first integral on the right-hand side can be recognized as a cross-correlational form of seismic interferometry. Since $\mathbf{x}_1$ is outside and $\mathbf{x}_2$ is inside of boundary S, this integral gives the time-reverse of the Green's function between $\mathbf{x}_1$ and $\mathbf{x}_2$. We replace this integral by the appropriate Green's function, move it to the left-hand side, and use source-receiver reciprocity such that $G^*_{ln'}(\mathbf{x},\mathbf{x}') = G^*_{n'l}(\mathbf{x}',\mathbf{x})$, allowing Eq. (A4) to be rewritten as

$$G_{im}(\mathbf{x}_2,\mathbf{x}_1) - G^*_{im}(\mathbf{x}_2,\mathbf{x}_1)$$
$$= \int_S \left\{ G_{in}(\mathbf{x}_2,\mathbf{x}) n_j c_{njkl} \partial_k \left[\int_{S'} \{G^*_{n'l}(\mathbf{x}',\mathbf{x}) n_{j'} c_{n'j'k'l'} \partial_{k'} G_{l'm}(\mathbf{x}',\mathbf{x}_1) - n_{j'} c_{n'j'k'l'} \partial_{k'} G^*_{l'l}(\mathbf{x}',\mathbf{x}) G_{n'm}(\mathbf{x}',\mathbf{x}_1)\} dS' \right] \right.$$
$$\left. - n_j c_{njkl} \partial_k G_{il}(\mathbf{x}_2,\mathbf{x}) \left[\int_{S'} \{G^*_{n'n}(\mathbf{x}',\mathbf{x}) n_{j'} c_{n'j'k'l'} \partial_{k'} G_{l'm}(\mathbf{x}',\mathbf{x}_1) - n_{j'} c_{n'j'k'l'} \partial_{k'} G^*_{l'n}(\mathbf{x}',\mathbf{x}) G_{n'm}(\mathbf{x}',\mathbf{x}_1)\} dS' \right] \right\} dS. \tag{A5}$$

This is an integral that describes the recovery of a homogeneous Green's function between a source at $\mathbf{x}_1$ and a receiver at $\mathbf{x}_2$ in elastic media. This is the elastic equivalent of Eq. (9) of the main text. While in the main text we have considered approximations allowing for simplified forms of the acoustic integrals, we have not shown the same here. However, such simplification is possible, albeit in a more complicated manner than for the acoustic case, requiring separation of *P*- and *S*-wave source types. For more details on such approximations see Wapenaar and Fokkema [19]. In Appendix B we show how formulas may be derived for different source and receiver configurations, and by extension of the elastic derivation presented here, it is also possible to derive similar relationships for the elastic case.

APPENDIX B: REPRESENTATION THEOREMS AND INTERFEROMETRIC INTEGRALS

A second representation theorem and interferometric formula related to those in Oristaglio [26] but for nonscattered fields can be obtained using the geometry shown in Fig. 1(b). In this case both source location $\mathbf{x}_1$ and receiver location $\mathbf{x}_2$ lie inside surface S of sources, and surface S is itself surrounded by surface S' of receivers. In this case, two correlational reciprocity theorems are used for states A, B, and C in Eqs. (1) and (2) [i.e., Eq. (1) is replaced by a reciprocity relation]. The same boundary conditions are used as in Eqs. (3) and (4) resulting in two representation theorems of correlation type [Eq. (3) is replaced by another correlational form]. Following a similar substitution to above [Eq. (4) into the replaced Eq. (3)], another representation theorem is obtained

$$p^*(\mathbf{x}_2) = -\int_V G(\mathbf{x},\mathbf{x}_2) q^*(\mathbf{x}) dV + \frac{-1}{j\omega\rho} \int_S \left\{ -\left[\int_{V'} G(\mathbf{x}',\mathbf{x}) q^*(\mathbf{x}') dV' \right] n_i \partial_i G(\mathbf{x}_2,\mathbf{x}) + n_i \partial_i \left[\int_{V'} G(\mathbf{x}',\mathbf{x}) q^*(\mathbf{x}') dV' \right] G(\mathbf{x}_2,\mathbf{x}) \right.$$
$$+ \left[\frac{-1}{j\omega\rho} \int_{S'} \{p^*(\mathbf{x}') n_{i'} \partial_{i'} G(\mathbf{x}',\mathbf{x}) - n_{i'} \partial_{i'} p^*(\mathbf{x}') G(\mathbf{x}',\mathbf{x})\} dS' \right] n_i \partial_i G(\mathbf{x}_2,\mathbf{x})$$
$$\left. - n_i \partial_i \left[\frac{-1}{j\omega\rho} \int_{S'} \{p^*(\mathbf{x}') n_{i'} \partial_{i'} G(\mathbf{x}',\mathbf{x}) - n_{i'} \partial_{i'} p^*(\mathbf{x}') G(\mathbf{x}',\mathbf{x})\} dS' \right] G(\mathbf{x}_2,\mathbf{x}) \right\} dS. \tag{B1}$$

Similarly to the previous derivation, to obtain an interferometric relation we define the remaining source term to be $q(\mathbf{x}) = \delta(\mathbf{x}-\mathbf{x}_1)$ and hence the pressure to be $p(\mathbf{x}) = G(\mathbf{x},\mathbf{x}_1)$. The second line of Eq. (B1) is then a convolutional interferometric integral with both $\mathbf{x}_1$ and $\mathbf{x}_2$ within the boundary; in this configuration the convolutional integral is exactly zero [19]. Hence, we obtain

$$G(\mathbf{x}_2,\mathbf{x}_1)+G^*(\mathbf{x}_2,\mathbf{x}_1)=\frac{-1}{j\omega\rho}\int_S\left\{\left[\frac{-1}{j\omega\rho}\int_{S'}\{G^*(\mathbf{x}',\mathbf{x}_1)n_{i'}\partial_{i'}G(\mathbf{x}',\mathbf{x})-n_{i'}\partial_{i'}G^*(\mathbf{x}',\mathbf{x}_1)G(\mathbf{x}',\mathbf{x})\}dS'\right]n_i\partial_iG(\mathbf{x}_2,\mathbf{x})\right.$$
$$\left.-n_i\partial_i\left[\frac{-1}{j\omega\rho}\int_{S'}\{G^*(\mathbf{x}',\mathbf{x}_1)n_{i'}\partial_{i'}G(\mathbf{x}',\mathbf{x})-n_{i'}\partial_{i'}G^*(\mathbf{x}',\mathbf{x}_1)G(\mathbf{x}',\mathbf{x})\}dS'\right]G(\mathbf{x}_2,\mathbf{x})\right\}dS. \tag{B2}$$

Equation (B2) gives a second acoustic interferometric relation that allows source-to-receiver Green's functions to be constructed using only Green's functions from surrounding sources and to surrounding receivers, in the geometry shown in Fig. 1(b).

A third such result can be derived for the geometry in Fig. 1(c) by starting with two convolutional reciprocity relations in place of Eqs. (3) and (4), and following similar steps in the derivation. The resulting representation theorem is

$$p(\mathbf{x}_2)=\int_V G(\mathbf{x},\mathbf{x}_2)q(\mathbf{x})dV+\frac{-1}{j\omega\rho}\int_S\left\{\left[\int_{V'}G(\mathbf{x}',\mathbf{x})q(\mathbf{x}')dV'\right]n_i\partial_iG(\mathbf{x}_2,\mathbf{x})-n_i\partial_i\left[\int_{V'}G(\mathbf{x}',\mathbf{x})q(\mathbf{x}')dV'\right]G(\mathbf{x}_2,\mathbf{x})\right.$$
$$+\left[\frac{-1}{j\omega\rho}\int_{S'}\{p(\mathbf{x}')n_{i'}\partial_{i'}G(\mathbf{x}',\mathbf{x})-n_{i'}\partial_{i'}p(\mathbf{x}')G(\mathbf{x}',\mathbf{x})\}dS'\right]n_i\partial_iG(\mathbf{x}_2,\mathbf{x})$$
$$\left.-n_i\partial_i\left[\frac{-1}{j\omega\rho}\int_{S'}\{p(\mathbf{x}')n_{i'}\partial_{i'}G(\mathbf{x}',\mathbf{x})-n_{i'}\partial_{i'}p(\mathbf{x}')G(\mathbf{x}',\mathbf{x})\}dS'\right]G(\mathbf{x}_2,\mathbf{x})\right\}dS. \tag{B3}$$

In reaching Eq. (9) of the main text we assumed that the regions outside of the boundary for the convolution integral were source free, and this resulted in volume terms being equal to zero. For the case considered in Eq. (B3) we use a similar assumption, resulting in the terms $q(\mathbf{x})$ and $q(\mathbf{x}')$ being equal to zero and the volume integral disappearing. It then follows that to obtain the source-receiver interferometric relation we define the pressure to be $p(\mathbf{x})=G(\mathbf{x},\mathbf{x}_1)$ giving

$$G(\mathbf{x}_2,\mathbf{x}_1)=\frac{-1}{j\omega\rho}\int_S\left\{\left[\frac{-1}{j\omega\rho}\int_{S'}\{G(\mathbf{x}',\mathbf{x}_1)n_{i'}\partial_{i'}G(\mathbf{x}',\mathbf{x})-n_{i'}\partial_{i'}G(\mathbf{x}',\mathbf{x}_1)G(\mathbf{x}',\mathbf{x})\}dS'\right]n_i\partial_iG(\mathbf{x}_2,\mathbf{x})\right.$$
$$\left.-n_i\partial_i\left[\frac{-1}{j\omega\rho}\int_{S'}\{G(\mathbf{x}',\mathbf{x}_1)n_{i'}\partial_{i'}G(\mathbf{x}',\mathbf{x})-n_{i'}\partial_{i'}G(\mathbf{x}',\mathbf{x}_1)G(\mathbf{x}',\mathbf{x})\}dS'\right]G(\mathbf{x}_2,\mathbf{x})\right\}dS. \tag{B4}$$

Equation (B4) gives a third acoustic interferometric relation that allows source-to-receiver Green's functions to be constructed using only Green's functions from boundary sources to surrounding receivers, in the geometry shown in Fig. 1(c).

[1] J. Rickett and J. Claerbout, The Leading Edge **18**, 957 (1999).
[2] O. Lobkis and R. Weaver, J. Acoust. Soc. Am. **110**, 3011 (2001).
[3] R. L. Weaver and O. I. Lobkis, Phys. Rev. Lett. **87**, 134301 (2001).
[4] M. Campillo and A. Paul, Science **299**, 547 (2003).
[5] D. Draganov, K. Wapenaar, and J. Thorbecke, Geophysics **71**, SI61 (2006).
[6] A. Bakulin and R. Calvert, Geophysics **71**, SI139 (2006).
[7] E. Slob, D. Draganov, and K. Wapenaar, Geophys. J. Int. **169**, 60 (2007).
[8] R.-R. Lu, M. Willis, X. Campman, J. Ajo-Franklin, and M. Nafi Toksoz, Geophysics **73**, S63 (2008).
[9] D.-J. van Manen, J. O. A. Robertsson, and A. Curtis, Phys. Rev. Lett. **94**, 164301 (2005).
[10] D.-J. van Manen, A. Curtis, and J. O. A. Robertsson, Geophysics **71**, SI47 (2006).
[11] D.-J. van Manen, J. O. A. Robertsson, and A. Curtis, J. Acoust. Soc. Am. **122**, EL115 (2007).
[12] A. Curtis, H. Nicolson, D. Halliday, J. Trampert, and B. Baptie, Nature Geoscience **2**, 700 (2009).
[13] S. Dong, R. He, and G. Schuster, *76th Annual International Meeting, SEG, Expanded Abstracts* (Society of Exploration Geophysics, Tulsa, OK, 2006), pp. 2783–2786.
[14] D. Halliday, A. Curtis, D.-J. van Manen, and J. O. A. Robertsson, Geophysics **72**, A69 (2007).
[15] D. Halliday, A. Curtis, and E. Kragh, The Leading Edge **27**, 210 (2008).
[16] D. Halliday and A. Curtis, Geophys. J. Int. **175**, 1067 (2008).
[17] D. Halliday and A. Curtis, Geophys. J. Int. **178**, 419 (2009).
[18] K. Wapenaar, Phys. Rev. Lett. **93**, 254301 (2004).
[19] K. Wapenaar and J. Fokkema, Geophysics **71**, SI33 (2006).
[20] K. Wapenaar, Geophysics **72**, SM5 (2007).
[21] K. Wapenaar, E. Slob, and R. Snieder, Phys. Rev. Lett. **97**, 234301 (2006).
[22] R. Snieder, K. Wapenaar, and U. Wegler, Phys. Rev. E **75**, 036103 (2007).
[23] M. Born and E. Wolf, *Principles of Optics* (Cambridge University Press, Cambridge, 1999).
[24] A. Curtis, 79th Annual International Meeting, SEG, Expanded Abstracts (Society of Exploration Geophyiscs, Tulsa, OK, 2009), pp. 3655–3658.

[25] J. Groenenboom and R. Snieder, J. Acoust. Soc. Am. **98**, 3482 (1995).
[26] M. L. Oristaglio, Inverse Probl. **5**, 1097 (1989).
[27] J. de Rosny and M. Fink, Phys. Rev. Lett. **89**, 124301 (2002).
[28] R. Snieder, Phys. Rev. E **69**, 046610 (2004).
[29] R. Snieder, K. Wapenaar, and K. Larner, Geophysics **71**, SI111 (2006).
[30] R. Snieder, K. van Wijk, M. Haney, and R. Calvert, Phys. Rev. E **78**, 036606 (2008).
[31] A. Curtis and D. Halliday, Geophysics **75**, SA1–SA14 (2010).
[32] D. Halliday and A. Curtis, Geophysics (to be published).
[33] I. R. Vasconcelos and R. Snieder, Phys. Rev. E **80**, 036605 (2009).
[34] R. Snieder, in *Scattering: Scattering and Inverse Scattering in Pure and Applied Science*, edited by R. Pike and P. Sabatier (Academic Press, 2002), Vol. 2, pp. 528–542.